Analysis of Resolution for an Amplitude Steered Array

Catherine H. Frazier [a], W. Jack Hughes [b], William D. O'Brien, Jr. [a]
[a] Bioacoustics Research Laboratory, Department of Electrical and Computer Engineering
University of Illinois at Urbana-Champaign, Urbana, IL 61801
[b] Applied Research Laboratory, The Pennsylvania State University
P. O. Box 30, State College, PA 16801

Abstract—
In 1976, Hughes and Thompson introduced the amplitude-steered array, which steered the maximum response of the linear array by amplitude weighting the output signals of the elements, thus eliminating the need for time delays or phase-shift networks. Currently that amplitude-steered array concept is being extended to a broadband two-dimensional array which can be used for real-time three-dimensional imaging. In shifting the use of the amplitude-steered array from underwater acoustic communications to imaging, we must consider different issues of the array's performance such as lateral and axial resolution. We show that both lateral and axial resolution are limited by the length of the array. The dependence of axial resolution on the length of the array is a unique feature of the amplitude-steered array, leading to an interesting tradeoff between lateral and axial resolution. We develop a theoretical basis for the dependence and give simulation results.

I. Introduction

Hughes and Thompson introduced the amplitude-steered array in 1976 [1]. The intent of amplitude steering was to tilt the maximum response of the beam pattern without using multiple delay lines or phase-shift networks, which are bulky. In their formulation, the beam was steered to a particular direction at a single frequency. The fact that the steering direction changed with frequency was considered a drawback of the design.

In this study, we use the change in steering direction with frequency to design a fast imaging system. By operating the amplitude-steered array in broadband mode with a chirp excitation, the maximum array response is swept over a range of angles. A sector can be scanned using a single transmit pulse, leading to fast two-dimensional imaging of the sector, compared to conventional imaging which uses at least one transmit pulse for each steering direction. A focusing lens can be placed in front of the array so that the steered beams are also focused in each direction.

The amplitude-steered imaging array possesses a unique quality that axial resolution is dependent on the length of the array. In fact, resolution in the lateral direction can be traded for resolution in the axial direction by changing the array length. With a conventional array, axial resolution is determined by the spatial length of the transmitted pulse, which can be related to the relative bandwidth of the transducer and the wavelength of the center frequency and is independent of the size of the transducer [2]. It is the unique relationship between axial and lateral resolution of the amplitude-steered array that is explored in this paper.

Section II gives a brief overview of amplitude steering and image formation using this array. We recommend that readers refer to [1] for a more complete discussion of amplitude steering. Section III describes the tradeoff between axial and lateral resolution. In Section IV, simulation results are presented. And in Section V, conclusions are given.

II. Amplitude Steering and Image Formation

We consider the one-way far-field pressure of a linear array of N equally spaced point receivers. To steer the maximum array response to θ_0, the signal from each element is phase-shifted by multiplying by the factor $e^{j(nk_0d\sin\theta_0)}$, where n is the element number, k_0 is the wavenumber at the design frequency and d is the distance between the elements. Then the pressure field is expressed as

$$P(r,\theta) = \frac{Ne^{jkr}}{r}H(\theta) = \frac{e^{jkr}}{r}\sum_i e^{-jnd(k\sin\theta - k_0\sin\theta_0)}. \quad (1)$$

The phase factor, $e^{j(nk_0d\sin\theta_0)}$, can be expressed as two weighting factors, $\cos(nk_0d\sin\theta_0)$ and $\sin(nk_0d\sin\theta_0)$. Conceptually to produce steering, the array of point sources could be operated first with cos weighting and then with sin weighting, then summing the two signal outputs with a 90° phase shift. In practice, the array layout is designed such that the cos and sin elements share the same space.

If the amplitude-steered array is excited by a frequency different from the design frequency used to calculate the weighting factors, the maximum response will occur at an angle different from θ_0, the designed steering direction.

$$k_0d\sin\theta_0 = kd\sin\theta_f \quad (2)$$

0-7803-5722-1/99/$10.00

Rearranging to solve for the new steering direction, θ, and substituting $k = 2\pi f/c$ gives

$$\theta_f = \sin^{-1}(\frac{f_0}{f}\sin\theta_0) \quad (3)$$

If the frequency increases, the angle that the beam is steered away from broadside decreases. An example of several beams from one array is shown in Figure 1. The 9.76-cm-length array is designed to steer to 5° at 5.6 MHz. Beams are shown for 5.6 MHz (5°), 4.5 MHz (6.23°), 3.4 MHz (8.25°), 2.3 MHz (12.25°), and 1.2 MHz (24°). As the frequency decreases, the beamwidths increase and the spacing between the beams also increases.

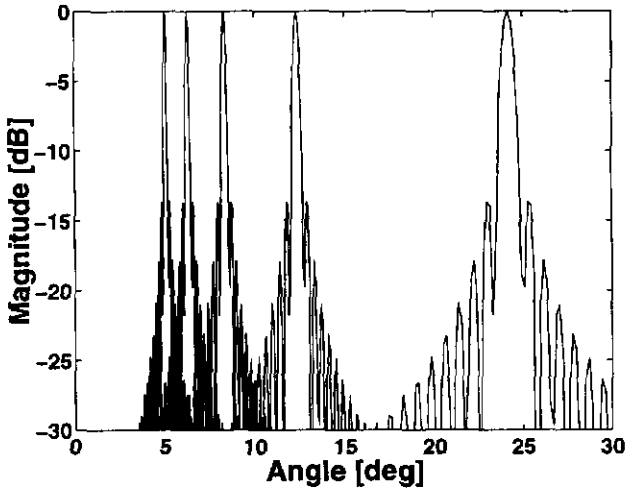

Figure 1: Beams from a 9.76-cm aperture steered to 5° at 5.6 MHz. Beams are shown for 5.6 MHz (5°), 4.5 MHz (6.23°), 3.4 MHz (8.25°), 2.3 MHz (12.25°), and 1.2 MHz (24°).

III. Axial and Lateral Resolution Tradeoff

For the purposes of this paper, resolution is defined as the -3 dB point spread function. Lateral resolution, in terms of angle, is calculated as

$$\alpha = \sin^{-1}(\sin\theta_0 + \frac{0.4423}{L}) - \sin^{-1}(sin\theta_0 - \frac{0.4423}{L}) \quad (4)$$

where $L = \frac{Ndf}{c}$ is the length of the array in terms of number of wavelengths. And axial resolution is calculated as

$$AR = 0.4423\, Q_{sig}\lambda \quad (5)$$

where Q_{sig} is the relative bandwidth of the received signal, $\frac{f_c}{\Delta_f}$. These equations are derived in [4].

The amplitude-steered array spatially separates frequencies by virtue of the fixed phase shift used to calculate amplitude weights. If the frequencies could be completely separated, *i.e.* beams were infinitely narrow, a point target would result in a single frequency return, which would imply that two points separated only in range could not be distinguished. Actually, it is possible to distinguish multiple targets in the same direction at different ranges because the beams are not infinitely thin, but overlap due to the finite length of the array.

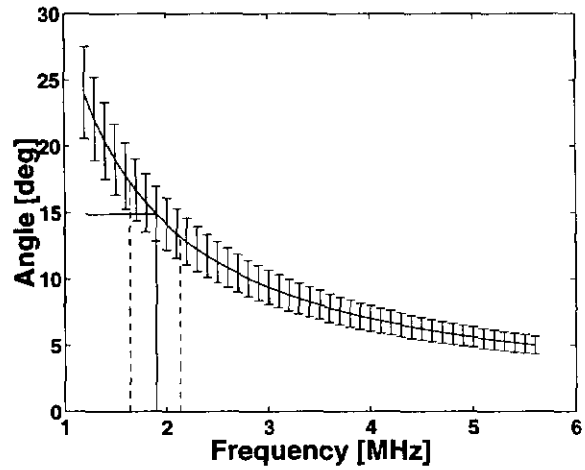

(a)

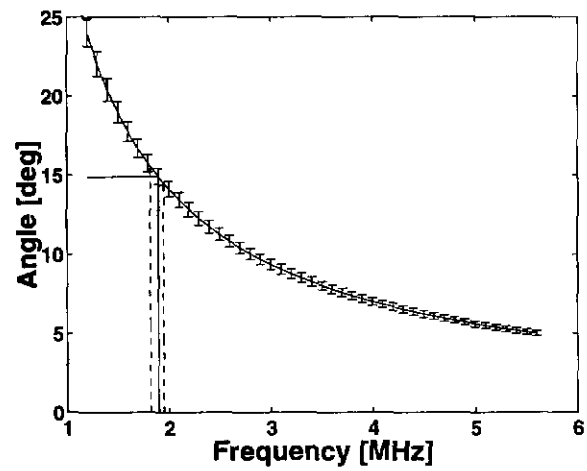

(b)

Figure 2: Lateral and axial resolution for (a) 1-cm-length and (b) 4-cm-length apertures. The line plotted is the steering direction versus frequency. The errorbars indicate the -3 dB beamwidth at each frequency.

Figure 2 conceptually shows the tradeoff between axial and lateral resolution. In each plot, the curve shows the steering direction versus frequency. The errorbars indicate the -3 dB beamwidth at each frequency. We can see from the errorbars that lateral resolution improves with increasing frequency.

Axial resolution can also be determined from this plot. At a particular steering direction, by observing the range of frequencies that overlap, we can determine the bandwidth at that particular direction. In the figures, this range is indicated by the dashed lines. Since, we know the center frequency from the line plotted, we know Q_{sig} and the wavelength. Axial resolution is then determined by Equation (5).

As frequencies decrease, the beamwidths increase, but the spacing between the beams also increases. The changes occur at such a rate that the relative bandwidth is approximately constant over the band of frequencies shown. Therefore axial resolution also improves with increasing frequency.

If the length of the aperture is increased from 1 cm to 4 cm, the lateral resolution improves. As shown in Figure 2b, relative to Figure 2a, the errorbars decrease. However, that decrease in beamwidth implies a decrease in the range of frequencies that overlap in a particular direction, illustrated by the more narrow range between the dashed lines. Therefore, relative bandwidth increases, and the axial resolution is worse.

IV. Simulation and Results

We analyze the tradeoff between axial and lateral resolution by simulating a linear array. The linear array has 452 elements with center-to-center spacing of 0.216 mm (9.76-cm-length aperture). The amplitude weighting is determined so that the main beam is steered to 5° at 5.6 MHz. The transmitted signal is a linear FM chirp with frequency swept from 1.2 MHz to 5.6 MHz.

The targets are placed at 20 m, well beyond the intended maximum range, so that they are in the far field for all steering directions. The speed of sound is assumed to be 1500 m/s for all simulations. Attenuation is not included. For comparison, we also simulate arrays with 694 elements (15-cm-length aperture) and 347 elements (7.5-cm-length aperture), but otherwise similar designs.

The array, operated in pulse-echo mode, receives an echo and the signals from all elements are summed to produce a single rf signal. To form a two-dimensional image, the received signal is first filtered with a matched filter for pulse-compression. Then the short-time Fourier transform (STFT) is calculated. The temporal position of the FFT window gives range information, and the frequencies contained in the window give lateral position information. The operation of the linear amplitude steered array has been simulated using the Field II program, developed by J. A. Jensen [5], [6]. Figure 3 shows an image of 6 point targets imaged using the 452-element array. We can immediately see that both axial and lateral resolution improve with decreasing steering direction, corresponding to increasing frequency.

In order to quantify the tradeoff between axial and lateral resolution, resolutions were measured from images of point targets. In addition to the resolution tradeoff that arises due to the length of the array, there is an additional tradeoff between axial and lateral resolution due to the processing. The

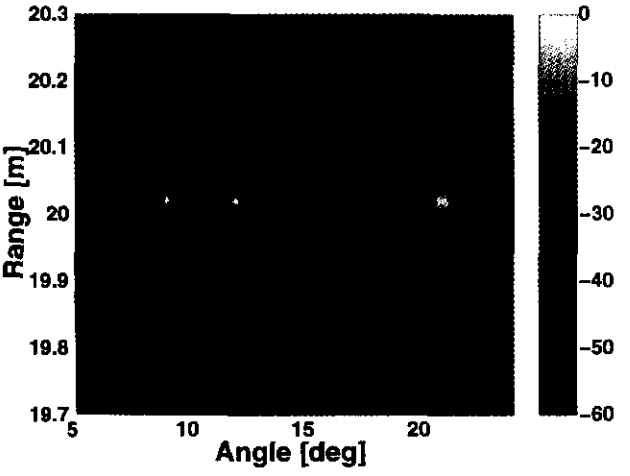

Figure 3: Image of 6 simulated targets.

length of the sliding FFT window affects both lateral and axial resolution of targets. A very short FFT window implies poor frequency resolution and therefore poor lateral resolution, but it also implies good time localization and therefore good axial resolution. The FFT window can be increased to improve lateral resolution until the fundamental limit on lateral resolution due to the length of the array is reached, but a long window means poor axial resolution.

Lateral and axial resolutions were measured from images formed using different length FFT windows in order to reduce the effect of processing on the measurements, so that we could measure the tradeoff in resolution due to the length of the array. Axial resolution was measured by setting the window length to be short, 8.333 μs. Lateral resolution was measured by setting the window length to be long, 0.147 ms. This window length was chosen by increasing the length of the FFT window until the improvement in lateral resolution at 6° was less than 0.5%. The image in Figure 3 is shown using a window length of 50.8 μs, which is a compromise between the two extremes.

Calculated and measured beamwidths and axial resolutions are shown in Figure 4 and Figure 5, respectively. From the figures, we can see that for all steering directions, lat-

eral resolution improves with increasing array length, and axial resolution degrades with increasing array length. Calculated beamwidths were found using Equation (4). Figure 4 shows that beamwidths measured from simulated data agreed with calculated beamwidths to a steering direction of 14°. At higher steering angles, corresponding to lower frequencies, the measured beamwidths were larger than calculated beamwidths. This agreement may be improved by using an even longer FFT window. Axial resolution was calculated using Equation (5), where the relative bandwidth, Q_{sig}, was calculated using the predicted beamwidths for each frequency and assuming a flat frequency response. Therefore a given frequency contributed to the bandwidth in each direction within the -3-dB beamwidth. Figure 5 shows that the calculated and measured axial resolutions agreed well.

The average Q_{sig} predicted for the 7.5-cm, 9.76-cm, and

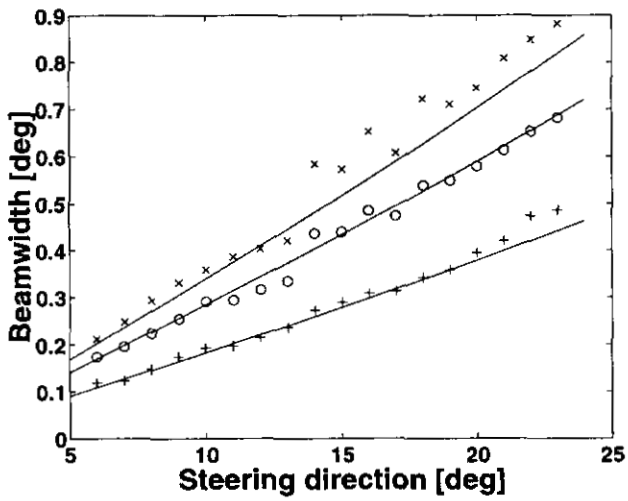

Figure 4: Comparison of calculated and measured beamwidths. Measured values are given for 7.5-cm length array (x), 9.76-cm length array (o), and 15-cm length array (+). Calculated values are indicated by the solid lines.

15-cm apertures are 27.60 ± 0.094, 35.90 ± 0.021, and 55.18 ± 0.054. The average Q_{sig} measured for the 7.5-cm, 9.76-cm and 15-cm apertures are 28.5 ± 1.85, 36.1 ± 2.01, and 54.1 ± 5.45, respectively.

V. Conclusions

The amplitude steered array is an array developed to decrease the complexity of electronics used to steer a beam. Data can be collected for a two-dimensional image with one transmit pulse, when the array is excited by a broadband pulse. When operated in this fashion, the axial resolution is dependent on the length of the array in terms of wave-

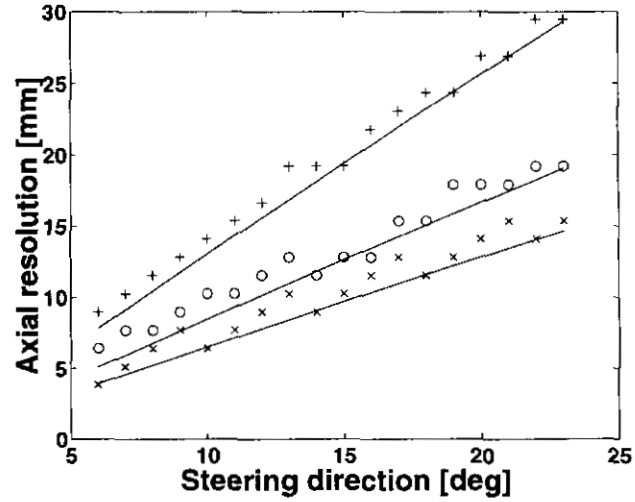

Figure 5: Comparison of calculated and measured axial resolutions. Measured values are given for 7.5-cm length array (x), 9.76-cm length array (o), and 15-cm length array (+). Calculated values are indicated by the solid lines.

length, which is different from the operation of conventional transducers.

Acknowledgements

This work was supported by DARPA under BAA 97-33.

References

[1] W. J. Hughes and W. Thompson, Jr., "Tilted directional response patterns formed by amplitude weighting and a single 90° phase shift," *J. Acoust. Soc. Am.*, vol. 59, no. 5, pp. 1040–1045, May 1976.

[2] D. A. Christensen, *Ultrasonic Bioinstrumentation.* New York: John Wiley and Sons, 1988.

[3] E. J. Skudrzyk, *The Foundations of Acoustics.* New York: Springer-Verlag, 1971.

[4] C. H. Frazier, W. J. Hughes, and W. D. O'Brien, Jr., "Analysis of resolution for an amplitude steered array," *J. Acoust. Soc. Am.*, submitted.

[5] J. A. Jensen, "FIELD: A program for simulating ultrasound systems," *Med. Biol. Engr. Comp.*, vol. 34, no. 1, Suppl. 1, pp. 351–353, 1996.

[6] FIELD II is available at the web site http://www.it.dtu.dk/~jaj/field/field.html